Diffusion of Octane in Silicalite: A Molecular Dynamics Study

Nilesh Raj,† German Sastre,‡ and C. Richard A. Catlow*

Davy Faraday Research Laboratory, The Royal Institution of Great Britain, 21 Albemarle Street, W1X 4BS London, U.K.

Received: April 21, 1999; In Final Form: September 24, 1999

Molecular dynamics simulations have been performed to study the diffusion of octane in silicalite. When hydrocarbons that are larger than C6 diffuse through this zeolite, the length of the molecule is such that diffusion through the sinusoidal channels becomes difficult. We have investigated the relative diffusivity through each channel and give an interpretation of the effect of temperature on this process. Simulations at 300 K show greater diffusivity in the sinusoidal channels, whereas at 450 K the straight channels show higher diffusion rates. When the temperature increases from 300 to 450 K, the diffusion coefficient in the straight channels increases by a factor of 5.2, whereas the coefficient in the sinusoidal channels increases by only 1.3. The trajectory plots also show larger diffusion paths through the straight channels at higher temperatures.

1. Introduction

In this paper we continue a series of studies[1,2] of the diffusion of hydrocarbons in zeolites using molecular dynamics (MD) simulation techniques. Our earlier work focused on the shape-selective diffusion of a range of aromatic hydrocarbons. Here we concentrate on octane, with the primary aim of elucidating its relative diffusivity in the different channels of zeolite ZSM-5.

Zeolites are microporous crystalline aluminosilicate materials that contain large pores and voids.[3,4] Both natural and synthetic materials are known. The zeolite framework is constructed from TO_4 interlinking tetrahedra, where T is a silicon or aluminum ion. The channels and intersections in zeolite frameworks have dimensions ranging from 3 to over 10 Å, enabling small and intermediate sized organic molecules to be accommodated.

One of the key characteristics of zeolites is their selective ability to adsorb guest molecules, due to their restricted internal structure which discriminates between adsorbates, depending on their size and shape. Selectivity may be enhanced by the presence of extraframework cations and protons, which are present due to the electrostatic imbalance that occurs when Si are replaced by Al ions.[4] The interest in zeolite research is in part motivated by their considerable importance in industrial processes. The largest area of application is as heterogeneous catalysts, where important zeolite catalyzed reactions are the conversion of methanol into gasoline;[5] isomerization;[6] and hydrocarbon synthesis. Other major industrial applications are in ion exchange[7] and gas separation.

Experimental studies of diffusivity of alkanes in zeolites have produced results with large discrepancies. For instance, frequency response techniques at 323 K for butane in silicalite gave a diffusivity of 1.0×10^{-6} cm^2/s[8], while membrane permeation at 334 K gave 3.7×10^{-8} cm^2/s[9]. Similar discrepancies have been reported for hexane.[10,11] A review of developments in the experimental study of intracrystalline diffusion in zeolites has been given by Ruthven,[12] who discusses possible explanations for the diverse set of results reported from microscopic methods (QENS and PFGNMR) and macroscopic methods.

In the present study we use the molecular dynamics (MD) technique as it allows direct simulation of time dependent processes such as diffusion. As discussed in ref 13, the basis of the technique is the integration of Newton's equations of motion, which yields considerable information on the system simulated but is computationally demanding. A number of approaches have been adopted to reduce computational expense and so allow longer simulation times. Among these are the fixing of the framework and the use of a simplified model for the guest molecules.[14] To justify the neglect of framework flexibility it is argued that the motions of zeolites and their guests are decoupled. The model has been used extensively and has successfully reproduced experimentally determined diffusion coefficients.[15−18]

Although the fixed framework model has been successful it is still a substantial departure from the real system, and removing this approximation is desirable for a more complete understanding of framework−guest interactions. The effect of framework flexibility has been included by Demontis et al.,[19] and Dumont and Bougeard.[20] It is expected that framework motions will assist in thermalizing sorbed molecules as is indeed observed by these authors. Results for methane in silicalite show the mean square displacement to be 20% smaller for the fixed framework simulations than for a flexible one. Framework flexibility was also included in the simulations of methane and ethene in silicalite by Catlow et al.[21] Their results for the self-diffusion coefficient are in reasonable agreement with experiment. The temperature dependence of diffusion is included in the work of Kawano et al.,[22] who also report good agreement for the results of the flexible framework model with experiment.

In the sections that follow we report our MD studies of diffusion of octane in silicalite. The size of the system with fully flexible framework and guest molecules is among the largest yet reported in the field of MD simulations of zeolites. In addition to the number of atomic species explicitly considered

* To whom correspondence should be addressed.

† Current address: Hitachi Europe Limited, Whitebrook Park, Lower Cookham Road, Maidenhead, SL6 8YA U.K.

‡ Current address: Instituto de Tecnologia Quimica U. P. V.-C. S. I. C., Universidad Politecnica de Valencia, Avenida Los Naranjos s/n, 46022 Valencia, Spain.

10.1021/jp991314f CCC: $18.00
Published on Web 11/30/1999

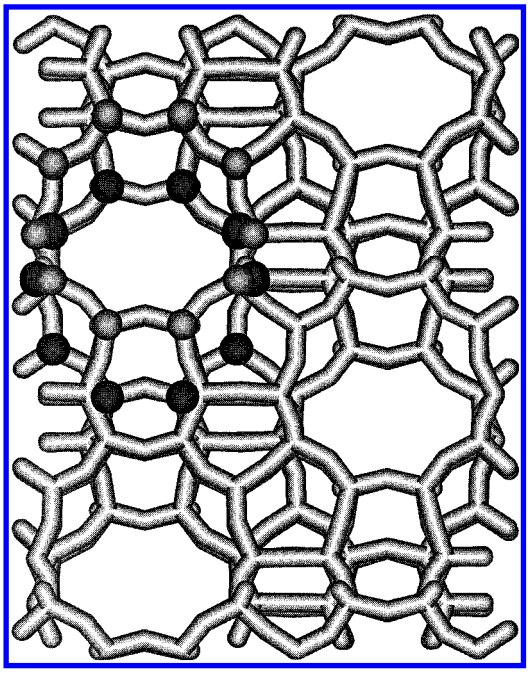

Figure 1. View of the orthorhombic silicalite through the sinusoidal channel. The channels are parallel to the [100] direction, and its tortuosity is shown by the different orientations of the 10 member rings (MR) along the channel directions. Two different 10 MR windows are highlighted in different shading to show this effect.

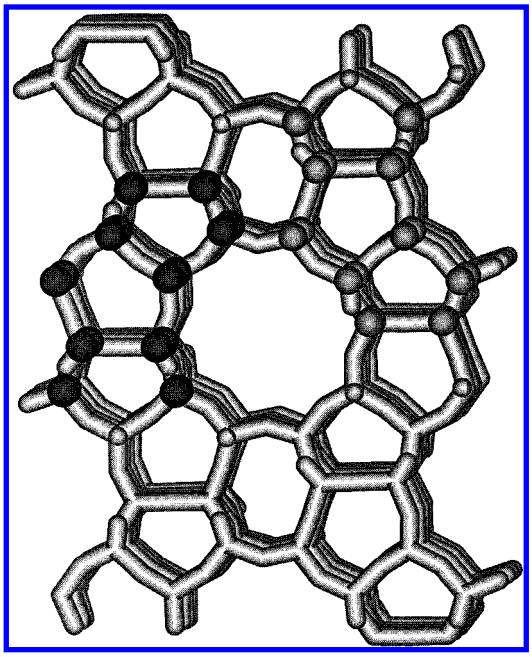

Figure 2. View of the orthorhombic silicalite through the straight channel, which is parallel to the [010] direction. The two 10 MR windows forming part of the sinusoidal channels shown in Figure 1 are also highlighted to emphasize the tortuosity of the sinusoidal channels.

we also use a detailed force field, details of which are given in section 2; while in section 3 we present our results for octane diffusion at 300 and 450 K. Finally, section 4 summarizes the main conclusions of this study.

2. The Model System

2.1. Structural Data. Silicalite has an orthorhombic structure[23] with unit cell dimensions $a = 20.022$ Å, $b = 19.899$ Å, and $c = 13.383$ Å, and space group *Pnma*. It belongs to the pentasil family of zeolites, so-called because it is formed from five-membered oxygen rings. The overall three-dimensional structure of silicalite has sinusoidal channels along [100] (Figure 1) and straight channels along [010] (Figure 2). Both channel systems are formed from 10-membered rings. The different forms of the channels give rise to anisotropic self-diffusion of adsorbed species. Our MD cell comprises $3\times3\times3$ unit cells of silicalite giving a total of 7776 framework atoms.

TABLE 1: Functional Form of the Zeolite Force Field Taken from Ref 24

Coulombic

$E_{ij} = q_i q_j / r_{ij}$

Four-Range Buckingham Potential

$E_{ij} = A \exp(-r_{ij}/\rho_{ij})$	$r_{ij} < r_1$
$E_{ij} = A_5 (r_{ij})^5 + A_4 (r_{ij})^4 + A_3 (r_{ij})^3 + A_2 (r_{ij})^2 + A_1 (r_{ij}) + A_0$	$r_1 \le r_{ij} < r_2$
$E_{ij} = B_3 (r_{ij})^3 + B_2 (r_{ij})^2 + B_1 (r_{ij}) + B_0$	$r_2 \le r_{ij} < r_3$
$E_{ij} = -C/(r_{ij})^6$	$r_3 \le r_{ij} \le r_c$
$E_{ij} = 0$	$r > r_c$

Exponential Three-Body

$E_{ijk} = (1/4) A_{ijk} (B_{ijk})^2 \exp(-r_{ij}/\rho_1) \exp(-r_{ik}/\rho_2)$

where

$A_{ijk} = K_{ijk}/2(\vartheta_e - \pi)^2$

$B_{ijk} = (\vartheta_e - \pi)^2 - (\vartheta - \pi)^2$

TABLE 2: Functional Form and Parameters of the Zeolite−Hydrocarbon and Hydrocarbon−Hydrocarbon Intermolecular Force Field Taken from Ref 25

Short Range Potentials

Lennard-Jones $E_{ij} = B_{ij} (r_{ij})^{-12} - C_{ij} (r_{ij})^{-6}$

Interaction	B_{ij} (eV Å^{12})	C_{ij} (eV Å^6)
C···O	1.1000×10^4	17.654
H···O	1.5564×10^3	5.5717
C···C	1.9692×10^4	18.0933
C···H	2.8000×10^3	5.8415
H···H	3.8484×10^2	1.9867

TABLE 3: Parameters and Functional Form of the Intramolecular Hydrocarbon Force Field Taken from Ref 26

C−C Bonds

$E_b = (1/2) K_b (r - r_o)^2$

where

$K_b = 41.48$ eV Å^{-2}

$r_o = 1.536$ Å

C−C−C, H−C−C, H−C−H Angles

$E_a = (1/2) K_a (\vartheta - \vartheta_o)^2$

where

$K_a = 3.39$ eV rad^{-2}

$\vartheta_o = 109.47$ degrees

2.2. Force Field and Parameters. As mentioned before, our MD simulations include framework flexibility, adsorbate flexibility, framework−adsorbate interactions, adsorbate−adsorbate interactions, and intramolecular interactions. In the case of eight octanes in the macrocell, the simulation comprises 7984 atoms, all of which are treated explicitly.

The framework is described in terms of long range electrostatic interactions, a short range, pairwise Buckingham potential, and a harmonic exponential three-body term for O−Si−O triads. These potential forms, summarized in Table 1, and their corresponding parameters were developed by Vessal[24] for the study of amorphous silica. For computational efficiency, the four-range Buckingham potential was splined at r_1, r_2, and r_3 to have continuous energy and first and second derivatives. These potentials have been used by Catlow et al. in their MD studies of sorbed methane and ethene in silicalite[21] and in our earlier studies of diffusion in zeolites.[1,2]

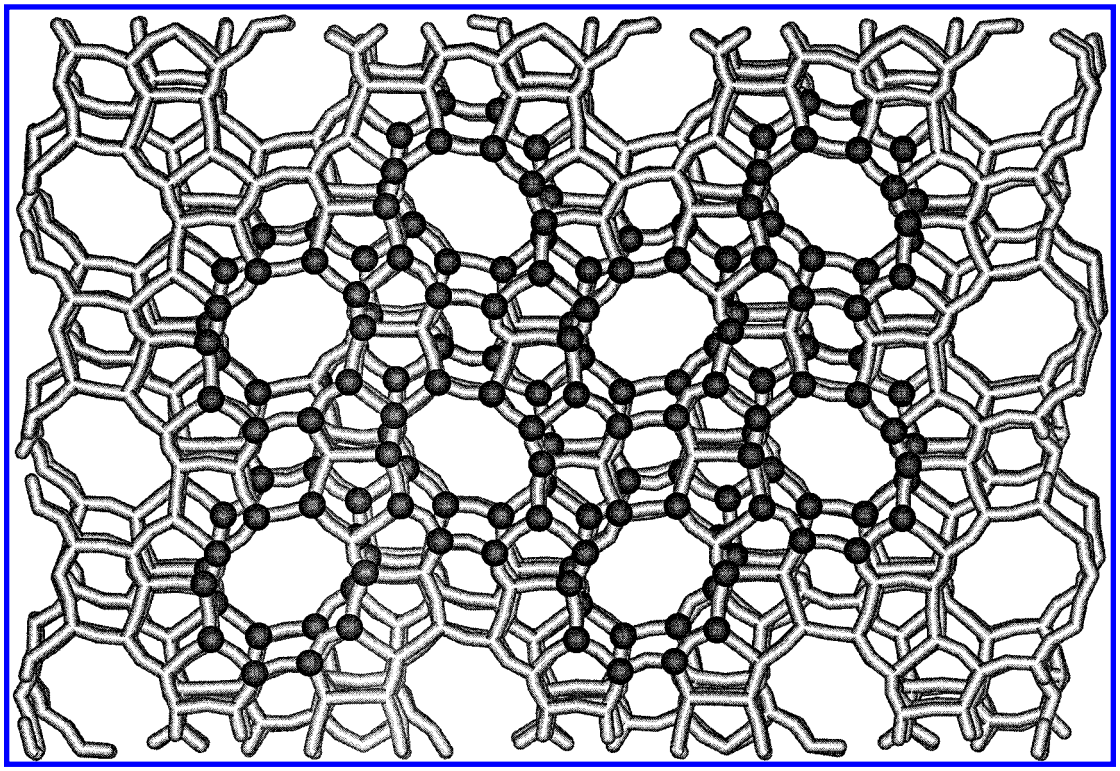

Figure 3. 3×3×3 silicalite macrocell after it has been minimized with the sorbate molecules inside (not shown). This view is parallel to [100] and it shows the sinusoidal channels whose 10 MR openings are highlighted.

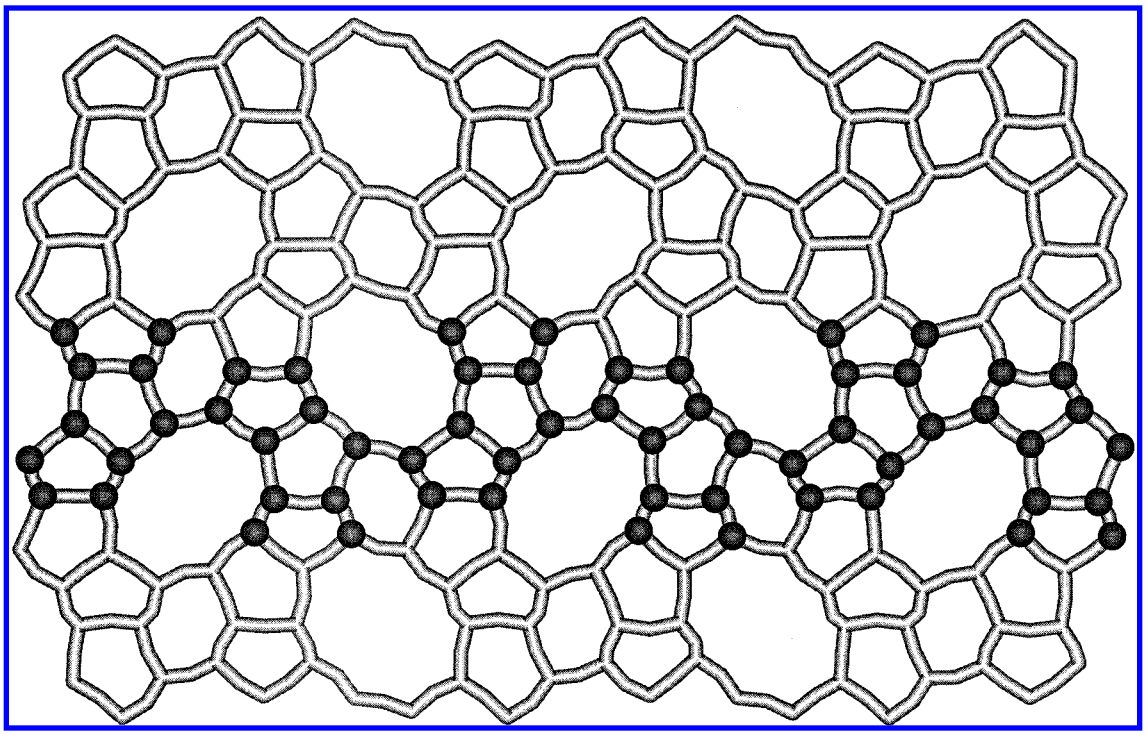

Figure 4. 3×3×3 silicalite macrocell after it has been minimized with the sorbate molecules inside (not shown). This view is parallel to [010] and it shows the straight channels. It is clear from this figure that the phase change from the orthorhombic structure (see Figure 2) to the monoclinic has affected the shape of the straight channels. Also, the 10 MR windows from one of the sinusoidal channels are highlighted to show its tortuosity.

Framework−guest and guest−guest interactions are described by a repulsive and an attractive term in the form of a Lennard-Jones potential (Table 2), and the parameters are taken from the work of Kiselev et al.[25] Only interactions between zeolite O ions and hydrocarbons are included, and, as is common practice, we neglect Si−guest interactions. Electrostatic interactions between zeolite ions and hydrocarbons are included, with carbon atoms being assigned a partial charge of −0.225 au and hydrogen atoms assigned a charge of +0.100 au, making the octanes charge neutral.

The force field for intramolecular hydrocarbon interactions is taken from ref 26. Bonds and bond-angle vibrations are described by harmonic potentials, details of which are given in Table 3. In the simulations, C−H bonds are constrained using

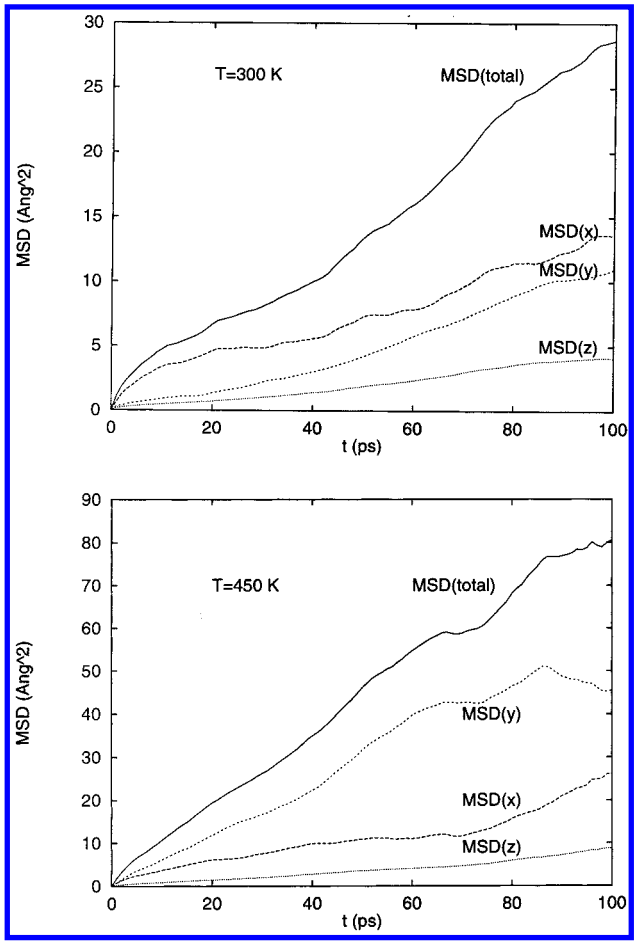

Figure 5. MSD plots obtained from the 100 ps runs at 300 K (top) and 450 K (bottom). The overall plots as well as the contributions from each axis direction, *x*, *y*, and *z*, are shown. The diffusion coefficients obtained from these plots using eq 2, are in Table 4.

the SHAKE algorithm with the constraint value being 1.054 Å. Interactions involving 1−4 pairs are described by a potential that is half the value of the full 12−6 Lennard-Jones energy. Interactions beyond 1−4 are described by the usual Lennard-Jones potential. Electrostatic interactions are included only for interactions beyond 1−4 pairs.

2.3. Simulation Procedure. The starting point for our simulations was the silicalite unit cell from the reported structure.[23] A supercell of dimensions 3×3×3 with respect to the unit cell was built and then energy minimized using the GULP[27] lattice modeling software. We did not locate octanes randomly inside the silicalite; instead, the molecules were placed inside the straight channels, avoiding strong contacts with each other and with the walls of the zeolite cage. Once the octane molecules were introduced into the macrocell, the structure was again energy minimized. On inserting the molecules, a transition to a monoclinic cell was observed as reported in the literature.[28−30] Although the transition is a consequence of thermal motions, the same effect can be also induced at lower temperatures by interactions between the zeolite framework and sorbed molecules matching the channel dimensions. In such cases the strong host−guest interactions result in the atomic motions leading to the phase transition. Our observation is therefore in accord with the experimental results, justifying the monoclinic cell observed in the simulations. The aspect of the channels, both sinusoidal and straight, changed as a result of this phase transition (Figures3 and 4). This structure was then used as the starting configuration for the MD simulations.

TABLE 4: Diffusion Coefficients (cm²/s) for Octane Obtained from the Plots of Figure 5

	D (cm²/s)
$T = 300$ K	
total	4.67×10^{-6}
x-direction	1.98×10^{-6}
y-direction	1.95×10^{-6}
z-direction	0.73×10^{-6}
$T = 450$ K	
total	13.87×10^{-6}
x-direction	2.53×10^{-6}
y-direction	10.23×10^{-6}
z-direction	1.09×10^{-6}

The molecular dynamics simulations were performed using the DL_POLY[31] code on an MPP Cray-T3D supercomputer. DL_POLY is a general purpose MD code that has been developed to run on a wide variety of computer architectures, including workstations and MPP supercomputers. It has been used to model polymers, macromolecules, complex fluids, and solids. The parallel version is written in the replicated data form and uses standard message passing libraries as well as highly optimized hardware specific communications. The present simulations were primarily run using 128 processors.

In the system with eight octanes at a temperature of 300 K, we used an equilibration period of 17 ps, after which trajectories were stored to be used in the final analysis. The total length of the production run was 140 ps. This is a long simulation for the size of system used and allowed us to obtain acceptable statistics for time-averaged MSD (mean square displacement) plots for over 100 ps. During the simulation, history files were saved every 1000 steps (or every ps). Subsequent analysis used the MSD facility included in DL_POLY. The expression used to calculate the MSD plots was the following:[13]

$$\langle X^2(t)\rangle = 1/(N_m N_{to}) \sum_i \sum_{to} [X_i(t + t_o) - (X_i(t_o)]^2 \qquad (1)$$

where N_m is the number of diffusing molecules, N_{to} is the number of time origins used in calculating the average, and X_i is the coordinate of the center of mass of molecule *i*.

The diffusion coefficients, *D*, are then calculated using the Einstein relation:[13]

$$\langle X^2(t)\rangle = 6Dt + B \qquad (2)$$

where *t* is the simulation time and *B* is the thermal factor arising from atomic vibrations.

3. Results and Discussion

We first discuss the MD simulations performed at 300 K and subsequently the results from the higher temperature simulations at 450 K. The MSD plots are shown in Figure 5. We used only the first 100 ps of the simulation after equilibration to approximate a linear plot. From the slope of this approximately linear graph we estimate the diffusion coefficient as 4.67×10^{-6} cm² s^{-1}. In Figure 5 we resolve the MSD plots into three components, and we see that at 300 K diffusion is greater in the *x*-direction than in the *y*-direction, and least in the *z*-direction. These results are summarized in Table 4. They are slightly surprising, for we might expect that diffusion would be greater in the *y*-direction, that is, the direction of the straight channels. Although such is the case for butane and hexane,[18] when the size of the alkane increases it has been found that the alkanes locate preferentially in the sinusoidal channels,[32] which explains our finding that the straight channels are not preferred for diffusion at this temperature.

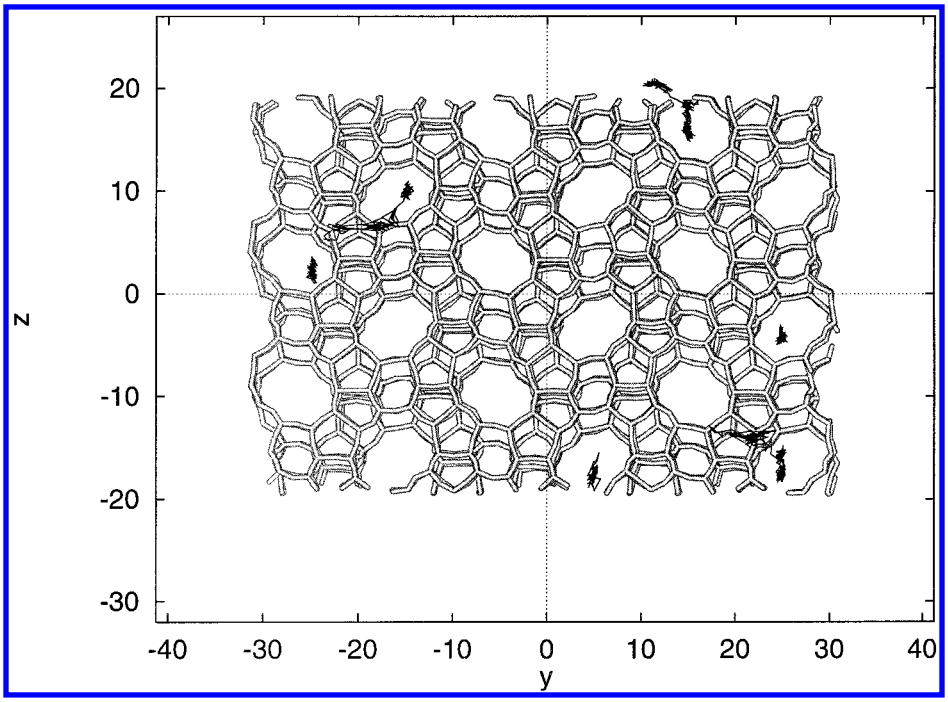

Figure 6. Trajectory plot showing the paths followed by the center of mass of the octane molecules in the 100 ps run at 300 K. The plot shows the trajectories in the *y*- and *z*-directions. The trajectories running along the *y*-direction correspond to diffusion through the straight channels. The sinusoidal channels are parallel to the *x*-direction (perpendicular to the plane of the paper), and we note that all of the octane molecules spend part of their time in some sinusoidal channels.

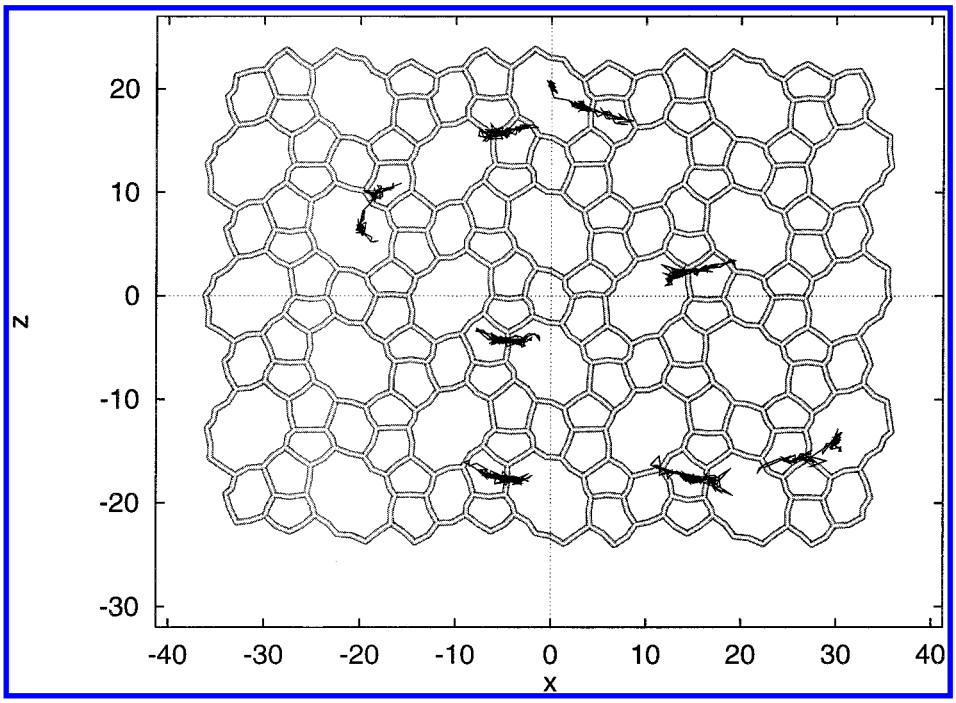

Figure 7. Trajectory plot showing the paths followed by the center of mass of the octane molecules in the 100 ps run at 300 K. The plot shows the trajectories in the *x*- and *z*-directions. The trajectories running along the *x*-direction correspond to diffusion through the sinusoidal channels. The straight channels are parallel to the *y*-direction (perpendicular to the plane of the paper), and we note that only three octane molecules spend part of their time in straight channels, located at the following (*x*, *z*) coordinates: (−20, 5), (0, 20), and (30, −15).

To aid further analysis of octane motion we have produced *trajectory* plots which show the diffusion paths along the sinusoidal (Figure 6) and the straight (Figure 7) channels for the 300 K simulation. These plots show the projections of the octane center-of-mass motions on the silicalite channels. They reveal that the motion of the molecules occurs more frequently in the sinusoidal channels. Thus in the projection parallel to the [010] straight channels shown in Figure 7, we find that only three octane molecules diffuse through this channel. To determine the time evolution of the octane motion, we give in Figures 8 and 9 *history* plots corresponding to the motions of each octane molecule in the *x*- and *y*-directions. By studying the plots in Figures 8 and 9, in conjunction with the trajectory plots, it is possible to gain a detailed understanding of the behavior of octane in silicalite. In Figures 8 (top) and 9 (top), we can compare octane mobility in the *x*- and *y*-directions at 300 K. It is seen that the mobility is lower in the *y*-direction, since this component (Figure 9, top) remains nearly constant

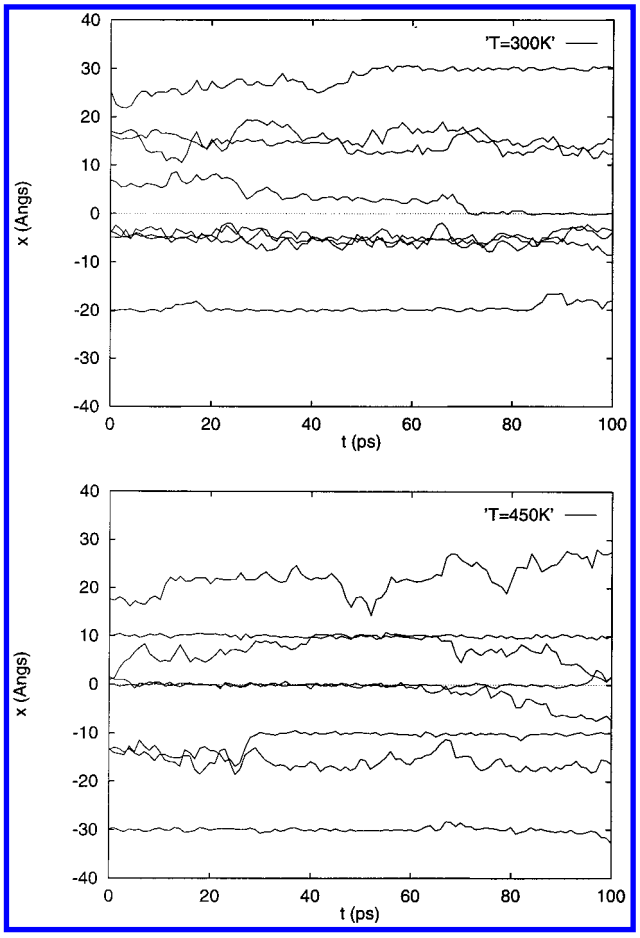

Figure 8. History plots showing the *x* center-of-mass coordinate evolution through the 100 ps runs at 300 K (top) and 450 K (bottom) for the eight octane molecules. The *x*-coordinate shows diffusion through the sinusoidal channels.

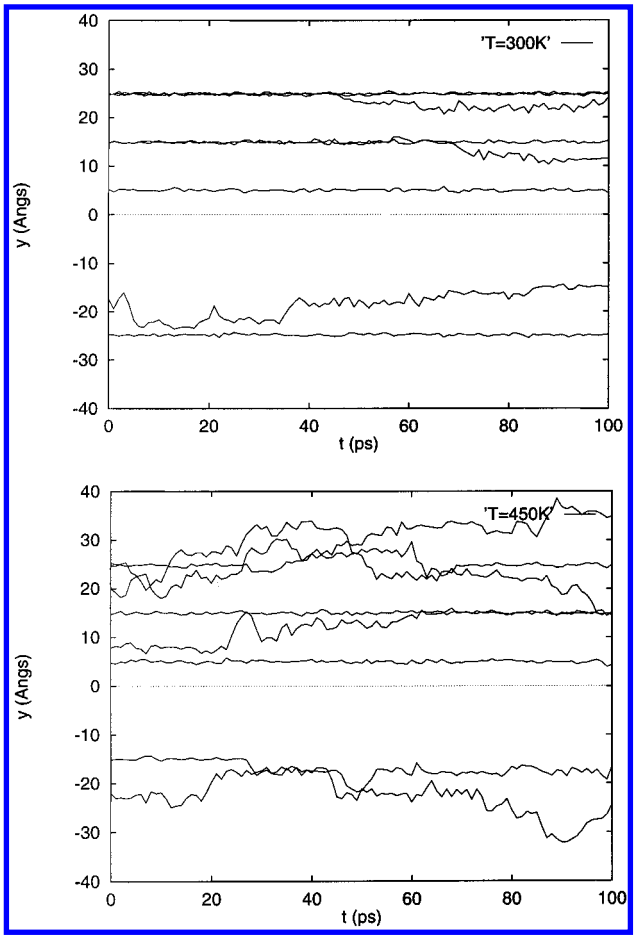

Figure 9. History plots showing the *y* center-of-mass coordinate evolution through the 100 ps runs at 300 K (top) and 450 K (bottom) for the eight octane molecules. The *y*-coordinate shows diffusion through the straight channels. We note from the plots that diffusion is more important at 450 K. It can be seen that at 300 K the coordinates of six octane molecules remain nearly constant through the 100 ps simulation.

for six of the octane molecules through the 100 ps simulation. Conversely the *x*-component (Figure 8, top) shows greater variations, indicating higher mobility in the sinusoidal channels.

We now compare these results with diffusion at the higher temperature of 450 K. Figure 5 (bottom) gives the MSD plot taken over 100 ps. In this case we have calculated the diffusion coefficients from the linear fit of the first 80 ps, owing to the lack of linearity in the final part of the plot. As expected, the diffusion coefficient obtained of 13.87×10^{-6} cm^2 s^{-1} is significantly higher than that at 300 K. Figure 5 also shows the *x*-, *y*-, and *z*-components of the MSD. In this case we see that the component of diffusivity is greater in the *y*-direction, which implies that the octane molecules are now also traversing the straight channels at this higher temperature. The component diffusion coefficients are given in Table 4. They show that a change in the mobility of octane has occurred at this temperature and now the straight channels are preferred with respect to the sinusoidal channels. We explain this below as being due to the different effect of the temperature on the octane mobility in each channel.

The history plots at 450 K (Figures 8 and 9, bottom) show that in this case there is noticeable mobility in both *x*- and *y*-directions, that is, the diffusion is taking place in both straight and sinusoidal channels. Simulation trajectory plots at 450 K (Figures 10 and 11) again depict octane motion through the sinusoidal and straight channels in silicalite. The salient feature here is that more molecules are able to pass between straight and sinusoidal channels. Figure 10 clearly shows a feature that is not observed in the simulations at 300 K, which consists of some long diffusion paths through the straight channels (diffusion in the *y*-direction). These long paths contribute to the higher diffusion coefficient in the straight channel. We note, however, that diffusion is also important in the sinusoidal channels as can be seen from Figure 11. Figure 11 also shows some evidence of *trapping* as octane molecules diffuse into the sinusoidal channels, the explanation for which may be that since these molecules are relatively long they are required to undergo significant conformational changes. For example, it may be necessary to rotate around the C−C bonds in such a way that the molecule adapts to the sinusoidal channel topology as it passes through it. Figure 12 shows the conformations of some octane molecules as they diffuse through the sinusoidal channels, and it can be seen how the molecules change the C−C−C−C dihedrals so as to adapt the octane skeleton to the topology of the channel. At higher temperatures such conformational changes need to occur more rapidly since diffusion is now much faster. This factor may help explain that when the temperature increases the octane molecules diffuse better through the straight channels where no conformational changes are necessary.

Our results are in accord with previous MD simulations of butane and hexane[16] where a similar increase in the diffusion coefficients in either channel system is found as the temperature increases. Moreover, from our simulations we conclude that the results of alkane diffusion should not be extrapolated to hydrocarbons of any size. When the length of the alkane is such

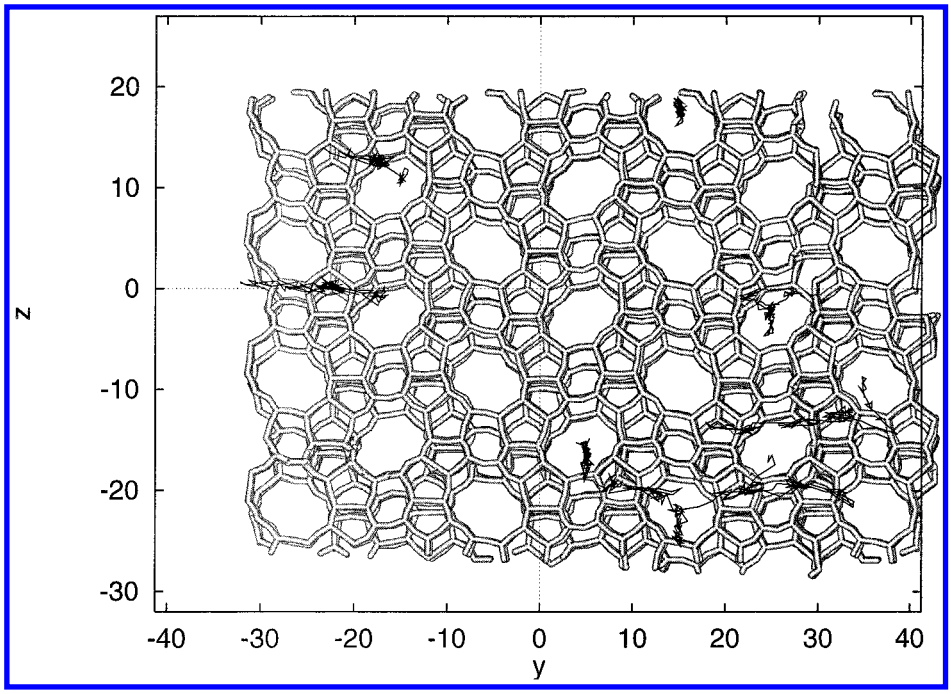

Figure 10. Trajectory plot showing the paths followed by the center of mass of the octane molecules in the 100 ps run at 450 K. The plot shows the trajectories in the *y*- and *z*-directions. The trajectories running along the *y*-direction correspond to diffusion through the straight channels. The diffusion through the straight channels is more pronounced than at 300 K, as can be seen from comparison with Figure 6.

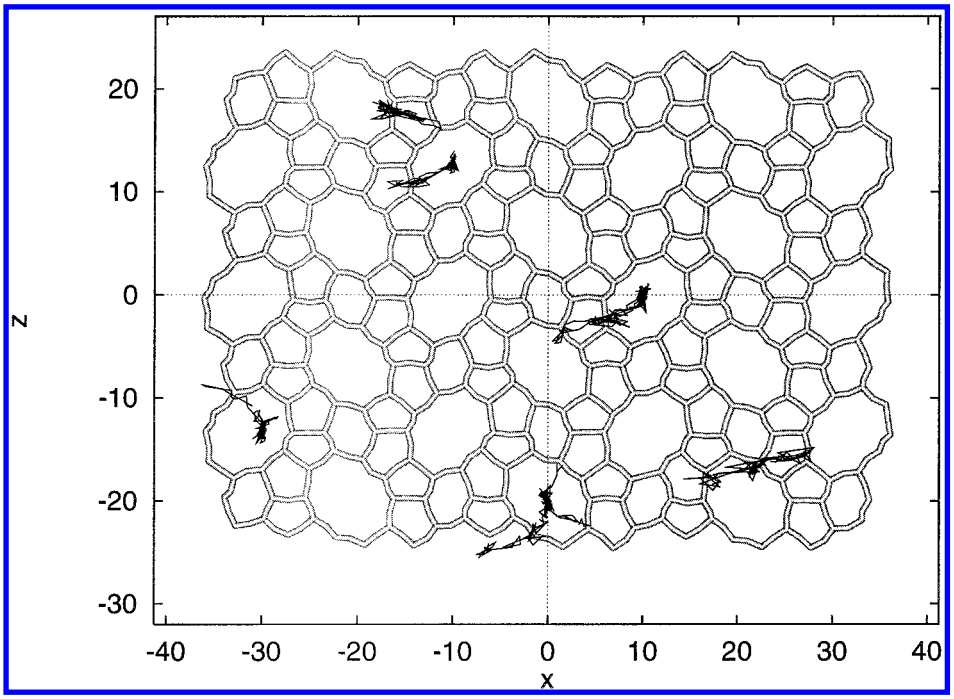

Figure 11. Trajectory plot showing the paths followed by the center of mass of the octane molecules in the 100 ps run at 450 K. The plot shows the trajectories in the *x*- and *z*-directions. The trajectories running along the *x*-direction correspond to diffusion through the sinusoidal channels. The straight channels are parallel to the *y*-direction (perpendicular to the plane of the paper), and we note from comparison with Figure 7 that at 450 K the straight channels are more populated and the sinusoidal channels are less populated.

that its diffusion through the sinusoidal channel involves considerable conformational changes in the C−C−C−C dihedrals, a different picture for the diffusion process emerges. In this sense octane is perhaps the first *n*-alkane where this effect starts to be noticeable, and this fact suggests careful comparison with data from smaller alkanes. The location of molecules in silicalite has been studied extensively and it is still a matter of debate, as shown in a recent study by Millot et al.,[32] where the authors find that octane tends to occupy different regions of silicalite from those occupied by smaller alkanes.

Our results are also comparable to the simulations using Brownian motion theory carried out by Maginn et al.,[33] where a diffusion coefficient of 8.5×10^{-6} cm^2 s^{-1} for octane at 300 K is reported. The same authors noted in a previous study[34] that octane is aproximately 8.8 Å long in its fully extended, all-trans conformation, and this distance is shorter than the distance between intersections along both straight and sinusoidal channels in silicalite. Residence in the straight channels allows chains to maintain close contact with the zeolite walls while keeping a nearly all-trans, thus minimum energy, conformation,

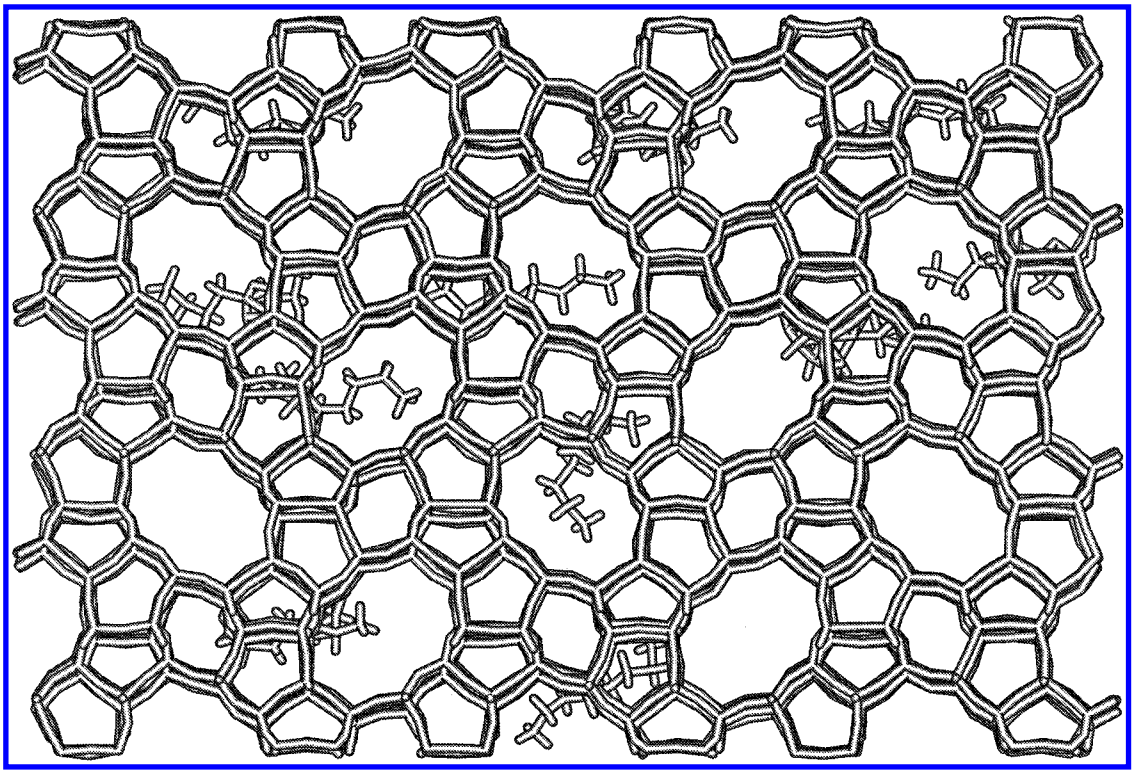

Figure 12. Conformations of some octane molecules taken from the simulation at 450 K showing the diffusion of octane molecules through the sinusoidal channels. The conformations correspond to different times in the simulation and have been superimposed in the same figure. We note that the molecules have to rotate along the C−C bonds in order to conform their orientation to the channel topology, making the diffusion somewhat restricted through these channels. The plane of the figure is perpendicular to the straight channels, which run along [010]; while the sinusoidal channels run along the plane of the figure, which corresponds to [100].

which can also occur in the sinusoidal channels when the octane molecules span only one segment of the sinusoidal channel; this will occur preferentially at lower temperatures, which explains the similarity of the diffusion coefficients along either channels at 300 K obtained in the present study. Our results also show, following this argument, that when the temperature increases, the diffusion coefficients increase in both channels, but the effect is more pronounced in the straight channels where there are fewer impediments to diffusion.

4. Conclusions

Our MD simulations show that the behavior of the octane molecule is very different from that of the smaller hydrocarbons previously studied. It is clear that when larger hydrocarbons diffuse through silicalite, the length of the molecules causes difficulties for the diffusion through the sinusoidal channels, due to the steric hindrance posed by the topology of the tortuous channels which interact differently with the ends of the linear molecules as they diffuse. This restriction forces the guest molecule to rotate along the C−C bonds so that the hydrocarbon skeleton adapts itself to the channel topology. The motions of internal rotation and diffusion through the sinusoidal channel have to couple appropriately for diffusion through these channels to proceed without appreciable steric restrictions. In this process temperature, therefore, plays an important role, as is clear from our simulations at different temperatures.

We found that flexible lattice calculations on the loaded zeolite reproduced the reported phase transition from the orthorhombic to the monoclinic crystal system. This transition is observed at the temperature of 350 K when no adsorbates are present, and is also induced, as we have seen, by the presence of sorbates. We found that at 300 K there is significant diffusivity of the octane molecules through the sinusoidal system. However, at 450 K we see comparatively more sorbate molecules diffusing through the straight channels, confirming that the equilibrium between octane molecules diffusing in each channel is temperature dependent. We predict a greater difficulty for the diffusion of octane through the sinusoidal channel as the temperature increases, which is due to the lack of coupling between internal hydrocarbon rotations and diffusion motions; or more simply, the internal rotation is not fast enough to accommodate for the higher diffusivity. The restrictions on the diffusion of the octane molecules through the sinusoidal channels appear, therefore, to be more important as the temperature increases, which is proved not only by the analysis of the trajectories made in this work but also by the individual diffusion coefficients calculated through each channel separately. In this sense, when the temperature increases from 300 to 450 K, the diffusion coefficient in the straight channels increases by a factor of 5.2, whereas the coefficient in the sinusoidal channels increases by only 1.3. The trajectory plots also show larger diffusion paths through the straight channels since in these channels there are not the diffusional restrictions for a long molecule that are present in the sinusoidal channels.

The present studies will be completed with a more detailed analysis of the temperature dependence on the nature of diffusion by performing longer simulations at still higher temperatures. Nevertheless, our current results already show an important and significant effect of the temperature on the diffusivity of octane molecules. The results and analyses of this MD study can also guide the interpretation of the diffusion features of larger *n*-alkanes.

Acknowledgment. G.S. thanks Ministerio de Educacion y Ciencia of Spain for a research contract. We thank Dr. W. Smith for useful discussions regarding DL_POLY code. The EPCC

(Edinburgh Parallel Computer Centre) and the EPSRC funded CRAY-T3D Materials Chemistry Consortium are gratefully acknowledged.

References and Notes

(1) Sastre, G.; Raj, N.; Catlow, C. R. A.; Roque-Malherbe, R.; Corma, A. J. *Phys. Chem. B* **1998**, *102*, 3198.

(2) Sastre, G.; Corma, A.; Catlow, C. R. A. *Top. Catal.* **1999**, *9*, 215.

(3) Catlow, C. R. A. In *Modelling of Structure and Reactivity in Zeolites*; Catlow, C. R. A., Ed.; Academic Press: London, 1992.

(4) Barrer, R. M. In *Zeolites and Clay Minerals as Sorbents and Molecular Sieves*; Academic Press: London, 1978.

(5) Meisel, S. L.; McCullough, J. P.; Lechthaler, C. H.; Weisz, P. B. *Chemtech*. **1976**, *6*, 86.

(6) Young, L. B.; Butter, S. A.; Kaeding, W. W *J. Catal.* **1982**, *76*, 418.

(7) Breck, D. W. In *Zeolite Molecular Sieves: Structure, Chemistry and Use*; Wiley and Sons: London, 1973, reprinted R. E. Krieger: Malabar, FL, 1984.

(8) van-den-Begin, N.; Rees, L. V. C.; Caro, J.; Bulow, M. *Zeolites* **1989**, *9*, 312.

(9) Hayhurst, D. T.; Paravar, A. R. *Zeolites* **1988**, *8*, 27.

(10) Beschmann, K.; Fuchs, S.; Riekert, L. *Zeolites* **1990**, *10*, 798.

(11) Wu, P.; Ma, Y. H. In *Proceedings of the 6th International Zeolite Conference*, Reno, NV, July 10−15, **1984**.

(12) Ruthven, D. M. *Stud. Surf. Sci. Catal.* **1995**, *97*, 223.

(13) Allen, M. P.; Tildesley, D. *Molecular Simulation of Liquids*; Oxford University Press: Oxford, 1980.

(14) Rickaert, J. P.; Bellemann, A.; Ciccotti, G.; Paolini, G. V. *Phys. Rev. A* **1989**, *39*, 259.

(15) Hufton, J. R. *J. Phys. Chem.* **1991**, *95*, 8836.

(16) Nowak, A. K.; den Ouden, C. J. J.; Pickett, S. D.; Smit, B.; Cheetham, A. K.; Post, M. F. M.; Thomas, J. M. *J. Phys. Chem.* **1991**, *95*, 848.

(17) June, R. L.; Bell, A. T.; Theodorou, D. N. *J. Phys. Chem.* **1992**, *96*, 1051.

(18) Hernandez, E.; Catlow, C. R. A. *Proc. R. Soc. London A* **1995**, *448*, 143.

(19) Demontis, P.; Suffritti, G. B.; Quartieri, S.; Fois, E. S.; Gamba, A. *Zeolites* **1987**, *7*, 522.

(20) Dumont, D.; Bougeard, D. *Zeolites* **1995**, *15*, 650.

(21) Catlow, C. R. A.; Freeman, C. M.; Vessal, B.; Tomlinson, S. M.; Leslie, M. *J. Chem. Soc., Faraday Trans.* **1991**, *87*, 1947.

(22) Kawano, M.; Vessal, B.; Catlow, C. R. A. *J. Chem. Soc., Chem. Commun.* **1992**, 879.

(23) van Koningsveld, H.; van Bekkum, H.; Jansen, J. C. *Acta Crystallogr.* **1987**, *B43*, 127.

(24) Vessal, B. *J. Non-Cryst. Solids* **1994**, *177*, 103.

(25) Kiselev, A. V.; Lopatkin, A. A.; Shulga, A. A. *Zeolites* **1985**, *5*, 261.

(26) Herzberg, G. In *Molecular Spectra and Molecular Structure*; van Nostrand: Princeton, 1950.

(27) Gale, J. D. *J. Chem. Soc., Faraday Trans.* **1997**, *93*, 629.

(28) Bell, R. G.; Jackson, R. A.; Catlow, C. R. A. *J. Chem. Soc., Chem. Commun.* **1990**, 782.

(29) Bouvier, F.; Weber, G. Sorption, Diffusion, and Separation in Microporous and Mesoporous Materials; Third FEZA Workshop, April 6−9, Manchester, U.K., 1997.

(30) Shah, D. B.; Guo, C. G.; Hayhurst, D. T. *J. Chem. Soc., Faraday Trans.* **1995**, *91*, 1143.

(31) Smith, W.; Forester, T. R. *J. Mol. Graphics* **1996**, *14*, 136.

(32) Millot, B.; Methivier, A.; Jobic, H. *J. Phys. Chem. B* **1998**, *102*, 3210.

(33) Maginn, E. J.; Bell, A. T.; Theodorou, D. N. *J. Phys. Chem.* **1996**, *100*, 7155.

(34) Maginn, E. J.; Bell, A. T.; Theodorou, D. N. *J. Phys. Chem.* **1995**, *99*, 2057.